Journal Pre-proof

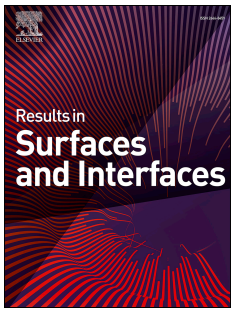

Utilizing Pomegranate Peel Biochar for Effective Malachite Green Adsorption

Zainab Haider Mussa, Ahmed Falah Imran, Lubna Raad Al-Ameer, Haider Falih Shamikh Al-Saedi, Issa Farhan Deyab, Fouad Fadhil A-Qaim, Hesam Kamyab

PII: S2666-8459(25)00205-3

DOI: https://doi.org/10.1016/j.rsurfi.2025.100618

Reference: RSURFI 100618

To appear in: *Results in Surfaces and Interfaces*

Received Date: 16 July 2025

Revised Date: 31 July 2025

Accepted Date: 5 August 2025

Please cite this article as: Mussa, Z.H., Imran, A.F., Al-Ameer, L.R., Al-Saedi, H.F.S., Deyab, I.F., A-Qaim, F.F., Kamyab, H., Utilizing Pomegranate Peel Biochar for Effective Malachite Green Adsorption, *Results in Surfaces and Interfaces*, https://doi.org/10.1016/j.rsurfi.2025.100618.

Our reference: RSURFI 100618

Article reference: RSURFI_RSURFI-D-25-00391

Article title: Utilizing Pomegranate Peel Biochar for Effective Malachite Green Adsorption

To be published in: Results in Surfaces and Interfaces

Title Page:

Utilizing Pomegranate Peel Biochar for Effective Malachite Green Adsorption

Zainab Haider Mussa[1], Ahmed Falah Imran[2], Lubna Raad Al-Ameer[3], Haider Falih Shamikh Al-Saedi[4], Issa Farhan Deyab[5], Fouad Fadhil A-Qaim[2*], Hesam Kamyab[6,7,8*]

[1]College of Biotechnology, Al-Qasim Green University, Al-Qasim, Iraq

[2]Department of Chemistry, Faculty of Science for Women, University of Babylon, PO Box 4, Hilla, Iraq

[3]College of Pharmacy, Al-Zahraa University for Women, Karbala, Iraq

[4]College of Pharmacy, University of Al-Ameed, Karbala, Iraq

[5]Medical Physics Department, Al-Mustaqbal University, 51001 Hillah, Babil, Iraq

[6]Faculty of Social Sciences, Media and Communication, University of Religions and Denominations, Pardisan, Qom, Iran

[7]Department of Biomaterials, Saveetha Dental College and Hospital, Saveetha Institute of Medical and Technical Sciences, Chennai 600 077, India

[8]The KU-KIST Graduate School of Energy and Environment, Korea University, 145 Anam-ro, Seongbuk-Gu, Seoul 02841, Republic of Korea

***Corresponding author's email:** fouad.fadhil@uobabylon.edu.iq; hesam_kamyab@yahoo.com

Utilizing Pomegranate Peel Biochar for Effective Malachite Green Adsorption

Abstract

The quest for efficient treatment technology has been spurred by the possibility that malachite green dye saturated wastewater may negatively impact both human health and the environment. Accordingly, this research was conducted to turn pomegranate peel into a biochar adsorbent for the elimination of malachite green that is spiked in water. Initial dye concentration, pH, contact time, volume of solution, and adsorbent dose were the five primary factors taken into consideration while designing all the tests. An amorphous structure was detected in the pomegranate peel activated carbon by XRD. Surface area was analyzed using BET for the specific surface area of 46.363 m^2/g. Scanning electron microscopy has been used to examine the surface characteristics, including porosity and cracks. At 200 mg/L, 16.3 mg, pH 7, and 100 min, the greatest dye removal efficiency and adsorption capacity of 99.85% and 362.6 mg/g were recorded under testing circumstances. The adsorption process was preferred to follow the Freundlich model with R^2 of 0.9996. Moreover, the pseudo-second-order model suited the data better than the other kinetic models. The homogeneous, monolayer surfaces driven by chemisorption were the nature of the adsorption, as demonstrated by the kinetics and isotherm analysis. Moreover, the research of thermodynamics demonstrated that adsorption is endothermic (+58.9 kJ/mol) and spontaneous ($\Delta G<0$). Finally, the regeneration of the adsorbent was investigated using four different eluents, and the potential for adsorbing other dyes was also evaluated. It can be concluded that industrial effluents could be effectively treated using the adsorbent material derived from pomegranate peel, as it is environmentally friendly, readily available, and possesses high adsorption capacity.

Keywords: Pomegranate peel; Adsorption-desorption; Malachite green; Adsorption isotherms; Kinetic studies

1. Introduction

Uncontrolled urbanization and industrialization have been identified as major contributors to environmental degradation and the depletion of natural resources. Large volumes of untreated wastewater are discharged into the environment owing to rapid industrial growth, urban expansion, and the unsustainable use of natural resources, placing significant pressure on freshwater supplies (Al-Qaim et al., 2018, 2017; Fadhil Al-Qaim et al., n.d.; Liu, 2021; Shah et al., 2021). Furthermore, the current state of the environment is comparable to that of the Anthropocene epoch in geological history, with human activity being largely responsible for the pollution of our planet today (Karaouzas et al., 2021). Therefore, measures to guarantee industrialization's sustainability are desperately needed, regarding both averting environmental harm (Abbood et al., 2023) and encouraging the growth of more ecologically friendly enterprises. The majority of water contamination is now caused by various organic, inorganic and microbial pollutants, which present serious problems for the environment and public health. These contaminants, originating from wastewater, freshwater sources, and other anthropogenic activities, are produced either naturally or artificially (Fito et al., 2022). However, because of the rapid growth of the textile industry driven by increasing demand for textile products, wastewater discharge has significantly increased, making the textile industry one of the major global sources of pollution. Wastewater from the textile sector contains a variety of contaminants, including heavy metals, biodegradable organics, laundry detergents, stabilizing agents, colorants, and desizers. Malachite Green (MG), a solid, cationic, crystalline dye, has the chemical name of 4-4-(dimethylamino)phenylmethylidene-N, N-dimethylcyclohexa-2,5-dien-1-

iminium chloride, with the chemical formula of $C_{23}H_{25}ClN_2$ and a molecular weight of 346.11 g/mol (Jabar et al., 2023; Oladoye et al., 2023). In addition, because of malachite's synthetic origin, increased stability, affordability, and superior water solubility, demand for it has grown across a range of industrial areas (Bhat et al., 2023; Lemos et al., 2023). It is widely used in the making of food, leather, textile dyeing, paint and pigment, wool, and silk, among other products (Bhat et al., 2023). Furthermore, aquaculture uses MG as a fungicide, parasiticide, and antiseptic (Abate et al., 2020). However, MG dye has negative effects on the environment and human health. MG is mutagenic, carcinogenic, teratogenic, persistent (resists natural bio-degradation), and bioaccumulative (He et al., 2023; Laskar et al., 2023; Merrad et al., 2023).

Moreover, swallowing MG in water poses no harm to the kidney, heart, or breast, all of which are essential human organs (Jabar et al., 2023). Drinking water contaminated with malachite is linked to diseases such as respiratory, gastrointestinal, and skin irritations (Merrad et al., 2023). Furthermore, leuco malachite (LMG), which is produced when MG is biochemically reduced in the human body system, raises liver tumours and promotes lung adenomas in males when it accumulates in the body for longer than five months (Oladoye et al., 2023). Aquatic life is endangered by the decrease in water surface oxygenation induced by the blockage of light flowing in, which is because of the discharge of sewage dyed with MG (Piriya et al., 2023). Some countries, including the United States, Canada, China, the United Kingdom, and the European Union, have outlawed the use of MG as a food coloring component (Barría et al., 2023). This is why the removal of persistent dyes, such as MG, has emerged as a critical task for the international community in order to preserve human health and the environment. Experts in the fields of environmental protection and public health now prefer innovative wastewater treatment procedures since conventional approaches have proven ineffectual in eliminating harmful and persistent contaminants such as MG dye. Researchers

have spent a great deal of time studying how to use cutting-edge wastewater technology to decolorize colored wastewater, for example, advanced oxidation process supported by UV irradiation (Jasim et al., 2024; Mohamed et al., 2011), membrane filtration (Izadmehr et al., 2020), and advanced oxidation method in the presence of a catalyst (Amigun et al., 2022; Mussa et al., 2024). These technologies have certain drawbacks, though, such as membrane technology's short lifespan and lack of sustainability due to dye molecules clogging filter pores and the inflated cost of acquisition (Lin and Zhang, 2023), capital intensiveness, complex chemistry tailoring, excessive oxidants needed to achieve the degradation process, large chemical requirements, and the production of excessively hazard sludge through materials deposition (Wang et al., 2021), as well as the unsupportable expense of both the investment and the high cost power source for electrochemical processes (Saravanan et al., 2022). Conversely, adsorption has emerged as a substitute pollution detoxification technique owing to its low cost, eco-friendliness, effectiveness, sustainability, and simplicity (Abdulhameed et al., 2025; Al-Asadi et al., 2025; Almuslem et al., 2023). Commercial activated carbon is well-known for its superior adsorption capacity and efficacy, and it is extensively used in a variety of industrial wastewater treatment sectors (Jabbar et al., 2022). Commercial activated carbon is effective and dependable, but its use is restricted by its non-sustainability and preparation costs (Fito et al., 2023). As a result, many researchers are still seeking adsorbents which are inexpensive and readily available locally. To avoid the drawbacks of commercial activated carbons, numerous research studies have been carried out on the creation of biomass-based adsorbent materials. To guarantee this, the effectiveness of adsorbent materials derived from agricultural waste (Abid et al., 2025; Al-Jaaf et al., 2022; Al-Qaim et al., 2024) in eliminating dyes is being studied. These materials are cheap, readily accessible, and easily usable. These investigations are limited by their poor adsorption capacity, high adsorbent consumption for small amounts

of adsorption, limited specific surface area, and lengthy contact times required for pollutant detoxification.

In this work, pomegranate peels were subjected to three physical processing steps: drying, crushing, and screening, which produced an effective MG adsorbent. The majority of pomegranate peels come from the byproducts of the pomegranate juice industry. Records show that processing one ton of pomegranate fruit yields approximately 669 kg of these byproducts (piths, rinds, and peels) (Hasnaoui et al., 2014). The peels and inner membrane of pomegranates make up an astonishing 50% of the entire fruit (Abdel-Salam et al., 2018). Pomegranate peels are widely accessible and contain several inherent functional groups that facilitate numerous processes and are crucial for pollutant adsorption. For instance, hydroxybenzoic (gallic and ellagic) acids, flavone derivatives, and hydroxycinnamic acids are responsible for their remarkable heavy metal chelation properties (Giri et al., 2021). A previous phytochemical investigation of pomegranate peels found ten phenolic compounds with a similar hexahydroxy diphenol moiety (Ruan et al., 2022). Tannins, phenolic acids, and flavonoids are the main phenolic substances that have been identified in pomegranate peels and reported in the literature (Singh et al., 2018). Pomegranate peels are considered a carbon-rich, inexpensive, and readily available material. They have been widely used in previous studies for the treatment of various pollutants, including dyes and metal ions. As a result, research on methods for preparing activated carbon from pomegranate peels has expanded significantly. These peels have been processed using various approaches, including 0.1 M HCl and 0.1 M NaOH (Abbasi et al., 2024), 80% phosphoric acid (1:1) (Waghmare et al., 2024), and NaOH (Genel et al., 2024). All of these methods have shown promising results in pollutant removal; however, differences have remained among the methods in regard to achieving optimal surface area and other desirable surface properties.

PPAC adsorbent has three main advantages: it is highly effective in removing dyes from aqueous solutions, readily available, and easy to obtain from plant sources. The study itself is simple to conduct in regard to batch experiments and adsorbent synthesis. Furthermore, dye analysis after adsorption does not require highly accurate instruments such as HPLC or LC/MS; instead, it can be performed using UV-visible spectroscopy. Despite the various advantages of activated carbon (AC) as an adsorbent, there are still limitations in its production process and challenges with regeneration, recycling capabilities, and selectivity toward specific contaminants. These limitations restrict its large-scale application in wastewater treatment. In addition, AC cannot simultaneously adsorb both cationic and anionic dyes unless its surface is modified.

2. Materials and methods

2.1. Materials

Merck supplied sulfuric acid, phosphoric acid, nitric acid, and potassium hydroxide as activating agents (All are analytical grade and used without further purification). MG ($C_{23}H_{26}N_2OCl$), a basic (cationic) dye, was used as the model adsorbate for adsorption studies. The dye was purchased from Dyestuffs and Chemicals Co., China, with a reported purity of 99%. Only analytical-grade chemicals were used, with no additional treatment required. However, several pretreatment experiments were conducted to select the most suitable activating agent, and potassium hydroxide (KOH) was ultimately chosen for subsequent experiments. The purity of all the materials was higher than 98%.

2.2. Adsorbent preparation

The pomegranate peel, used as the precursor material for the production of AC, was collected from local markets in Babylon, Iraq. The sample was thoroughly

washed with tap water and then rinsed with distilled water. After removing any dust, it was sun-dried, and residual moisture was eliminated by placing it in an oven at 80 °C for 24 h. Following oven drying, the peel was fully impregnated with phosphoric acid in a 1:1 (m/v) ratio. It was then dried again in the oven for 8 h before being pyrolyzed in a furnace at 350 °C for 2 h.

After cooling in a dry place, the resulting adsorbent material was thoroughly washed with distilled water until the pH reached neutral. Finally, AC was ground to a particle size of 750 μm and stored in a sealed plastic container until further use.

2.3. PPAC surface characterization

The adsorbent obtained from pomegranate peel was evaluated using various techniques, including Scanning Electron Microscopy (SEM), Brunauer–Emmett–Teller (BET) surface area analysis, Fourier Transform Infrared (FTIR) spectroscopy, and X-ray Diffraction (XRD). The crystalline structure and functional groups of the adsorbent material were determined using XRD (Bruker D2 Phaser) and FTIR (PerkinElmer Spectrum), respectively. The FTIR scan was conducted over a wavelength range of 400–4000 cm^{-1}. Furthermore, surface morphology and specific surface area were determined by BET and SEM (ΣIGMA, JSM-7610F, Carl Zeiss, Germany), respectively.

2.4. Experiments for adsorption of malachite green on PPAC

A 50 mL solution was used for the batch adsorption experiment to remove malachite green dye using an adsorbent derived from pomegranate peel. To prepare the dye solution, 100 milligrams of MG dye were dissolved in 100 mL of distilled water. Separate solutions with concentrations of 30, 60, 100, 200, and 300 mg/L were then prepared. The pH of the solutions was adjusted using 0.1 M NaOH and 0.1 M HCl to achieve the desired acidity or alkalinity. Subsequently, 50 mL of each MG dye solution was mixed with a suitable

amount of PPAC. The mixtures were then shaken for a specified contact time using an orbital shaker. After the contact period, the solutions were centrifuged at 3000 rpm to separate the supernatants. The amount of dye that remained in the aqueous solution was then determined using UV-visible spectroscopy. Ultimately, an ultraviolet (UV)-visible spectrophotometer (UH4150, Hitachi) with a maximum wavelength of 615 nm was used to calculate the final dye concentration after adsorption.

A stock solution of MG dye for the calibration curve development was prepared by weighing 100 mg of powdered MG dye and dissolving it in 100 mL of distilled water to obtain a 1000 mg/L dye solution. A calibration curve was then constructed using serial dilutions of the MG dye at the concentrations of 0.3, 0.5, 1, 2, 5, 15, and 25 mg/L. The standard solutions were placed in UV-VIS spectrophotometer cuvettes, and the maximum wavelength was set at 615 nm. The absorbance measurements for each sample were then recorded and documented in an Excel spreadsheet.

A calibration curve was obtained by plotting absorbance values (y-axis) against dye concentrations in mg/L (x-axis) to determine the best linear fit. The resulting linear equation was used to calculate unknown concentrations. Equations (1) and (2) were employed to calculate the removal efficiency and adsorption capacity, respectively:

$$\mathrm{R\%} = \frac{\mathrm{C_0} - C_t}{\mathrm{C_f}} \times 100 \qquad (1)$$

$$\mathrm{Q}_t = \frac{(\mathrm{C_0} - C_t)}{\mathrm{m}} \times \mathrm{V} \qquad (2)$$

where C_0 (mg/L) and C_t (mg/L) are the initial and residual concentrations of malachite green, respectively, R% represents the removal efficiency, Q_t is the adsorption capacity at time t, m is the mass of the adsorbent (g), and V is the volume of the solution (L).

2.5. Adsorption isotherm

Adsorption isotherms describe the interaction between the adsorbent and adsorbate at equilibrium. These equilibrium relationships also help us understand the fundamental adsorption mechanisms and the surface characteristics of both the adsorbent and the adsorbate. The most commonly used adsorption models are the Langmuir and the Freundlich isotherms, although other models can also represent adsorption behavior.

The Langmuir model assumes a monolayer adsorption on a homogeneous surface with strong interactions between the adsorbent and adsorbate. In contrast, the Freundlich model suggests a heterogeneous surface with multilayer adsorption. The Freundlich isotherm also indicates an enhancement of the adsorptive properties of the surface.

If the Langmuir model fits the data well, the adsorption is likely chemisorption; if the Freundlich model provides a better fit, the process is generally considered physical adsorption.

For the isotherm study, the initial dye concentration was varied (200, 300, 350, 400, and 450 mg/L), while pH (7), contact time (100 min), and adsorbent dosage (0.04 g) were kept constant. The Langmuir, Freundlich, and Dubinin-Radushkevich isotherm models are presented in Equations (3)–(5), respectively (Jani et al., 2024; Olasehinde et al., 2020):

$$\frac{C_e}{\mathrm{Q_e}} = \frac{1}{\mathrm{Q_m} K_L} + \frac{1}{Q_m} C_e \qquad (3)$$

$$\ln \mathrm{Q_e} = \ln \mathrm{K_f} + \frac{1}{\mathrm{n}} \ln \mathrm{C_e} \qquad (4)$$

$$\ln \mathrm{Q_e} = ln Q_m - K_{ad} \varepsilon^2 \qquad (5)$$

where Ce is the concentration at equilibrium contact time, KL is the Langmuir constant associated with adsorption capacity, KF and n are Freundlich constants associated with adsorption intensity (Abbas and Trari, 2023), Q_m is the maximum Langmuir adsorption capacity, and K_{ad} is the constant that refers to sorption energy.

2.6. Adsorption kinetics

The possible rate-controlling phase in the adsorption process is identified by studying adsorption kinetics. Furthermore, it makes it possible to comprehend kinetic processes and the dye uptake rate. In the present work, the nature of the adsorption between AC generated from pomegranate peel and MG dye was investigated by analyzing the two commonly used kinetics models, i.e., Pseudo-first-order (PFO) and pseudo-second-order (PSO) kinetics. In addition, Weber-Morris intraparticle diffusion was investigated. PFO and PSO are frequently associated with chemisorption and physical adsorption, respectively. In the simplest possible way, chemical sorption results in a strong connection between the gently attaching adsorbent and the adsorbate. Conversely, during the rapid adsorption stage of physical adsorption, there are weak contacts between the adsorbent and adsorbate. Therefore, it is simple to reverse physical adsorption, but chemical adsorption is more difficult to reverse. For the kinetics investigation, the following parameters were used: pH 7, adsorbent dose of 0.04 g, beginning dye concentration of 100 mg/L, and varied contact periods of 3, 5, 10, 15, 30, and 60 min. Equations (6)–(8) provide the fundamental formulas needed to calculate PFO, PSO and Weber-Morris intraparticle diffusion, respectively:

$$\log(Q_e - Q_t) = \log Q_e - \frac{K_1}{2.303} t \qquad (6)$$

$$\frac{t}{Q_t} = \frac{1}{K_2 Q_e^2} + \frac{1}{Qe} t \quad (7)$$

$$Q_t = K_{diff}.\, t^{1/2} + C \quad (8)$$

where K1 and K2 are pseudo-first-order (min-1) and pseudo-second-order (g/(mg.min)) adsorption rate constants, respectively (Al-Asadi et al., 2023); Qt and Qe (mg/g) represent the adsorption capacity at time t and equilibrium adsorption capacity, respectively; K_{diff} is the rate diffusion constant, $t^{1/2}$ is the square root of the contact time, and C is the intercept (Wu et al., 2009).

2.7. Adsorption thermodynamics

The adsorption thermodynamics is important since it tells us whether the adsorption process is spontaneous or not. It also aids in determining the energy involved in the adsorption process, the endothermic or exothermic nature of the process, and the adsorption's feasibility. By varying the system's temperature, the adsorption of MG dye from a water-based solution was investigated thermodynamically (293, 303, 313, and 323K) while maintaining the other variables at their ideal levels (period time of 100 min, PPAC dosage of 0.04 g, and MG dye concentration of 200 mg/L). The thermodynamic variables, change in enthalpy (Δ°H), change in entropy (Δ°S), and change in Gibbs free energy (Δ°G) were determined using Equations (9)–(12):

$$\Delta G = -RT\ln Kd \quad (9)$$

$$Kd = \frac{Cs}{Ce} \quad (10)$$

$$\ln Kd = \frac{\Delta S}{R} - \frac{\Delta H}{RT} \quad (11)$$

$$\Delta G° = \Delta H° - T\Delta S° \quad (12)$$

where T is the absolute temperature (K), Kd stands for the thermodynamic constant, and R is the universal gas constant (8.314 J/mol. K). Ce is the

concentration of MG dye at equilibrium, Cs is the concentration of dye adsorbed (mg/L) on the adsorbent at equilibrium, and the symbols ΔG°, ΔS°, and ΔH° stand for the changes in Gibbs free energy, entropy and enthalpy, respectively. The values of ΔH° and ΔS° were determined using the slope and intercept from the plot between ln Kd and 1/T.

3. Results and discussion

3.1. PPAC characteristics

Using XRD, the crystalline nature of the AC derived from pomegranate peel was investigated. The outcome of the investigation is shown in **Figure 1a.** It is evident from the XRD examination that the adsorbent's overall structure is amorphous. The (002) plane of disordered carbon is typically responsible for the broad peak observed in AS XRD patterns, usually located between 18° and 26°. However, the PPAC adsorbent shows very small peaks, probably because of the addition of KOH during chemical activation. A faint peak observed around 38°–42° in the chemically activated PPAC sample corresponds to the (100) plane of graphitic carbon (Xing et al., 2023). In general, amorphous surfaces work better than crystalline structures for the adsorption of several pollutants that differ in size and structure (Kumar et al., 2014). Using the nitrogen gas adsorption-desorption concept, the BET-specific surface area of activated carbon derived from pomegranate peel was ascertained **(Figure 1b).** The apparatus 1and adsorption temperature were 0 and 77K, respectively. The mass sample used was 0.015 g. Simply said, the affinity for pollutant adsorption will essentially increase with the adsorbent's particular surface since there will be more active sites available at that surface (Raji et al., 2023). Generally, the surface area and type of the adsorbent material have a major influence on the rate of adsorption. Higher surface area materials have more adsorbing sites, which increases the amount of adsorption. Conversely, porous materials offer more surface area, which increases adsorption capacity and removal efficiency.

Essentially, the adsorbent's surface area is increased by finely splitting (powdering), which ultimately improves the adsorption effectiveness. It was discovered that the activated carbon pomegranate peel has a BET specific surface area of 46.363 m^2/g. In this investigation, the specific surface area measured is greater than that of the AC derived from waste fig leaves of 18 m^2/g, as reported in our previous study (Al-Asadi et al., 2023). SEM was used to analyze the produced adsorbent's morphology, and the results are shown in **Figure 1c.** The figure indicates that the adsorbent has a porous structure and holes that allow it to absorb different types of contaminants with different sizes and structures (Khadim et al., 2022). Because of the chemical and heat activation used to increase the AC's adsorption capacity (Ali et al., 2022), morphological fractures such as holes and uneven forms are seen. The pore size distributions of PPAC are presented in **Figure 1d**. As it can be observed, PPAC exhibits a pore size distribution centered between 4–12 nm, indicating a development of microporosity of the material (Wang et al., 2005). FTIR was effectively used to analyze the functional groups of activated carbon derived from pomegranate peel, both before and after adsorption, as shown in **Figure 1e**. It was discovered that the adsorbent was made up of many functional groups with the ability to absorb different contaminants of different sizes and structures (Humadi et al., 2023). The signal detected at 3423.26 cm^{-1} in the FTIR analysis of the activated carbon derived from pomegranate peel prior to adsorption is ascribed to –OH, which contains functional groups such as hydroxyl and water. The presence of C=O and C-O vibrations, which are characteristics of the carbonyl group extending from ketones and ethers, is responsible for the two distinct, strong peaks that can be seen at 1574.95 and 1421.99 cm^{-1}. A lesser peak, 1040.99 cm^{-1}, is connected to the C–H stretching action. Finally, the presence of C-H bending is shown by the peak at 650.21 cm^{-1}. Following MG loading, two more peaks that had developed at 1012.63 and 922.03 cm^{-1} disappeared. The FTIR spectra of the pollutant-loaded

activated carbon showed notable peak alterations compared to the pre-adsorption values. Following adsorption, peaks were shown to move and diminish. The observed significant shifts from before to after adsorption were as follows: 3423.26 cm^{-1} to 3396.35 cm^{-1}, 1574.95 cm^{-1} to 1573.54 cm^{-1}, 1040.99 cm^{-1} to 1039.58 cm^{-1}, and 650.09 cm^{-1} to 645.84 cm^{-1}. These shifts indicated the impact of carboxyl, O-H, C=O, C–H stretching, and C–H bending on the AC surface based on pomegranate peel during adsorption. In addition, two peaks—1012 and 922—vanish once MG is adsorbed on PPAC.

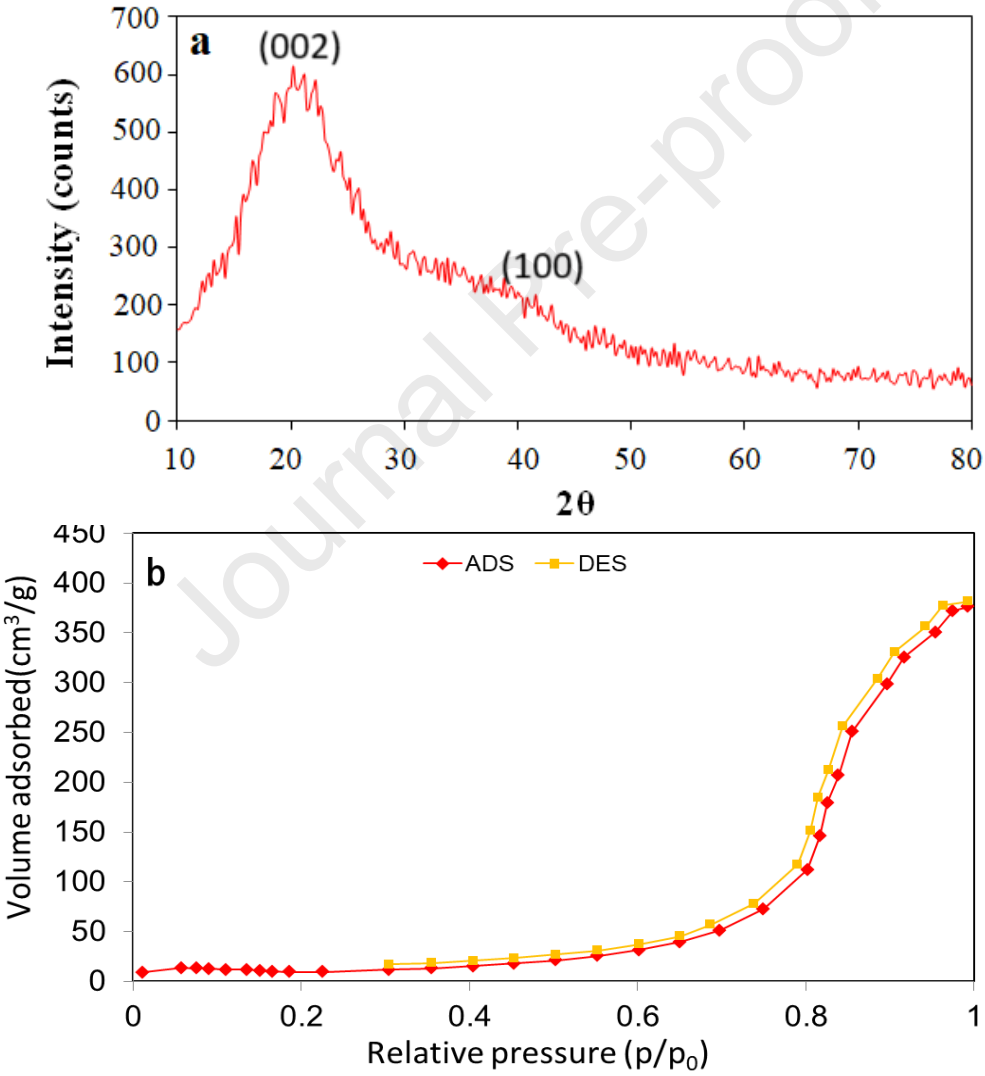

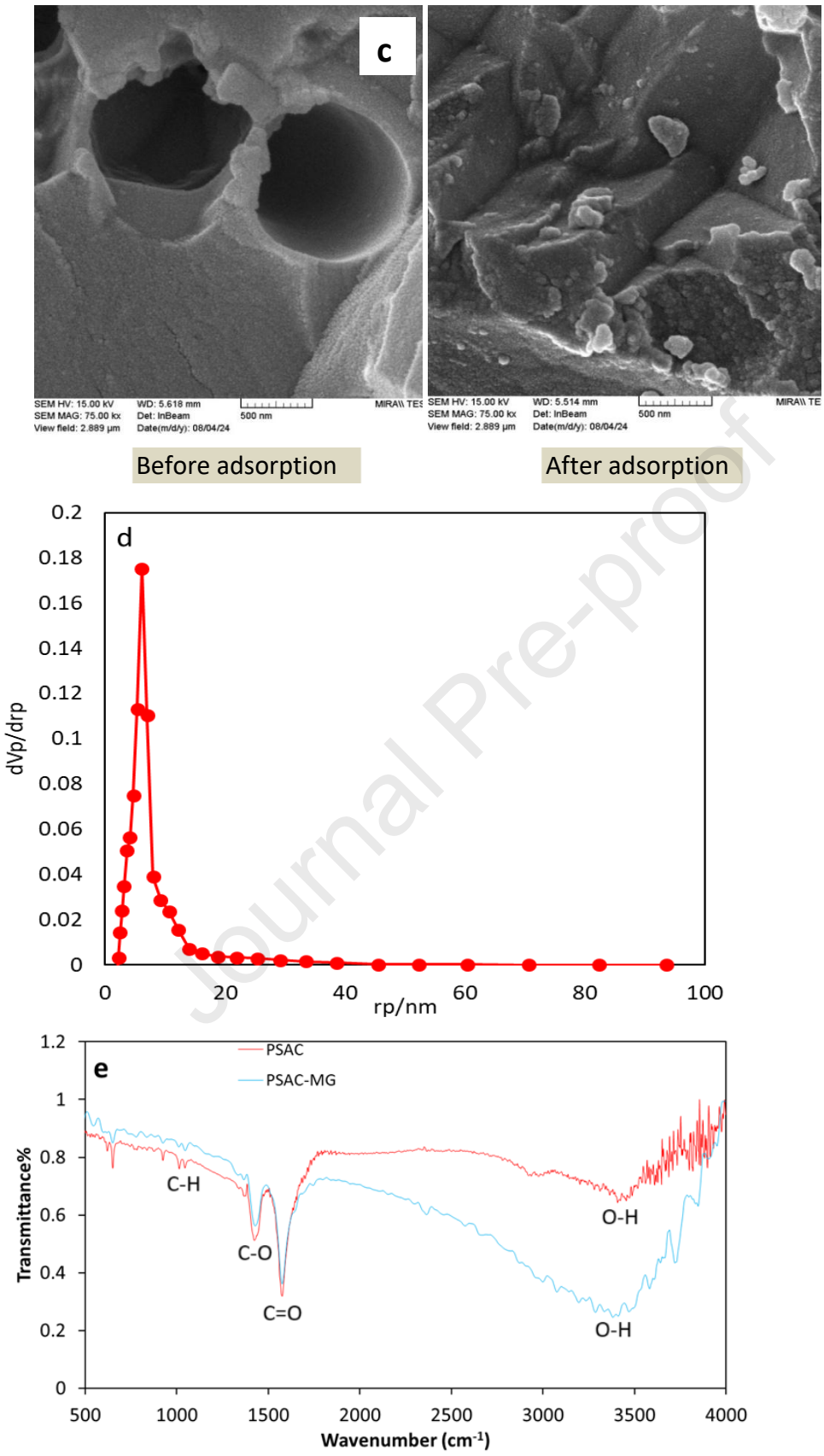

Fig. 1 Characterization of PPAC surface: **a** XRD spectrums of PPAC sample**; b** nitrogen adsorption–desorption isotherms**; c** micrographs of PPAC before and

after MG adsorption; **d** Pore size distribution (BJH model); **e** FTIR investigation of the most common identified functional groups for PPAC before and after MG adsorption

3.2. Batch adsorption performance

With the use of AC derived from pomegranate peel, MG dye was adsorbed from an aqueous solution in a batch manner. The adsorption efficiency and capacity of the PPAC adsorbent are displayed in **Table 1** under different testing conditions. The results of this investigation showed that the greatest and least removal efficiencies were, respectively, 99.85% and 9.4%. Under the ideal operating conditions of pH 11, a contact time of 100 minutes, an initial dye concentration of 100 mg/L, and an adsorbent dose of 0.04 g, the highest removal efficiency was achieved in this investigation. Conversely, under testing circumstances with pH, contact duration, dye concentration, and adsorbent dose of 3, 100 min, 100 mg/L, and 0.04 g, respectively, the lowest removal efficiency (9.4%) was measured. Generally, while evaluating the efficacy of various adsorbents on dye detoxification, a number of factors should be taken into account. These comprise the kind of wastewater (aqueous or actual), the activation mode (thermal, chemical, or both), the amount of adsorbent used, the particular surface area, the pollutant content, etc.

3.3. Effects of operating parameters

3.3.1. Effects of equilibrium time vs initial concentration

Figure 2 illustrates the investigation of the impact of varying contact periods (0-140 min) and initial concentration levels (30-300 mg/L), with a fixed adsorbent dosage, pH solution, and initial temperature, on the elimination of MG dye from pomegranate peel-AC.

The initial concentration of the MG dye has a significant role in the adsorption capacity by giving the dye molecules a stronger driving force to overcome mass

transfer resistances between the solid phases and aqueous solution (Ahmad Khan et al., 2023). As shown in **Figure 2**, a detailed study was conducted into the impact of activated carbon made from pomegranate peel on the adsorption of MG dye at different levels (30–300 mg/L). The effectiveness of dye adsorbed onto adsorbent material was found to be 98.3% at a concentration of 100 mg/L. The clearance, however, was reduced as the concentration of MG dye was increased; at 300 mg/L, the dye concentration reached a minimum of 30%. For the upcoming studies, the ideal concentration was determined to be 100 mg/L. The results showed that at a concentration of 200 and 300 mg/L, a low removal of the MG dye happened after 140 min (53 and 30.3, respectively), with an adsorption capacity of 132.5 and 113.6 mg/g, respectively. The main factor for the amount of MG dye absorbed onto the adsorbent material to rise with an increase in contact time is the abundance of open pores and holes on the pomegranate peel-AC adsorbent material. Furthermore, as time increases, the probability of dye molecules being adsorbed rises. Nevertheless, the removal efficiency decreased over the 100-minute contact period, indicating that equilibrium was reached.

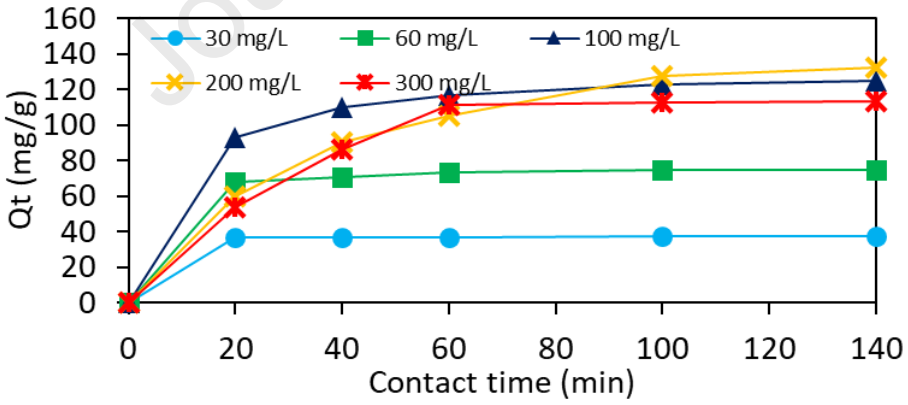

Fig. 2. Impact of the starting concentration (pH 7, 0.04 g adsorbent, 50 mL, (0-140) min) on the MG adsorption capacity (top) and removal efficiency (bottom) using PPAC

3.3.2. Effect of pH

As shown in **Figure 3** and **Table 1**, the impact of pH on the effectiveness of dye removal was investigated by adjusting the pH from pH 3 to pH 11. Because of the competition between the dye molecules and H^+ for accessible active sites at lower pH values, it was shown that reducing the pH and dye removal efficiency (Taqui et al., 2023). Because resistance is absent, cationic dyes such as MG are often greatly absorbed at higher pH levels. Here, at a pH of 11, the highest removal effectiveness of 99.85% was observed. Similarly, as **Figure 3** illustrates, the maximum adsorption capacity for the removal of dye was at pH 11, 124.8 mg/g. The removal efficiency and adsorption capacity were first reduced by lowering the pH solution, and they reached 9.4% and 11.75 mg/g, respectively, at pH 3. For further experiments, pH 8 was selected in order not to make further modifications to all MG dye solutions.

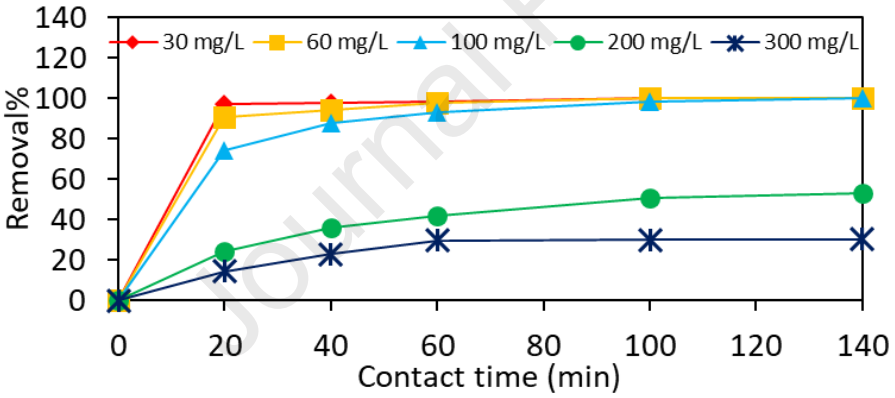

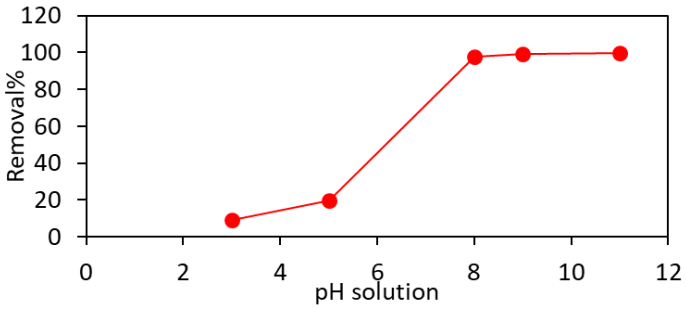

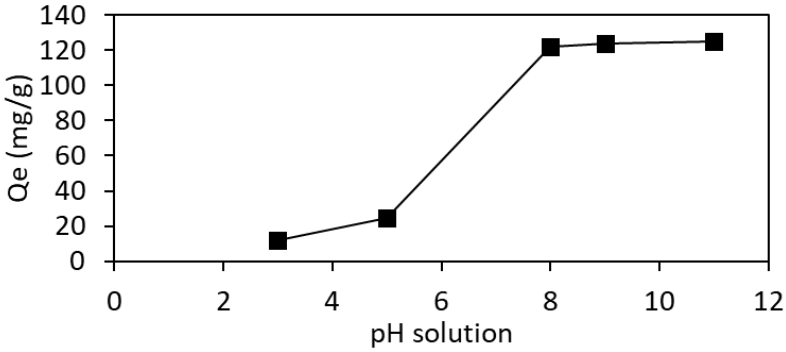

Fig. 3 Impact of pH solution on MG's adsorption capacity and removal efficiency using PPAC (100 mg/L MB, 0.04 g adsorbent, 50 mL, 100 min).

3.3.3. Effect of PPAC amount

The evaluation of the dose of AC derived from pomegranate peel for the adsorption of 200 mg/L of MG dye solution at pH 7 is presented in **Figure 4** and **Table 1**. The figure shows that the adsorption effectiveness of MG increased from 59.1% to 99.04% at PPAC doses of 0.0163 and 0.838 g, respectively. This is because of the increase in the quantity of accessible unoccupied adsorption sites and the surface area of the adsorbent for adsorption (Abuzerr et al., 2018). A large dosage of adsorbent may lead to high removal efficiency.

However, the adsorption capacity reduces as the dose rises. If the adsorbent dose is raised further, it may not be sufficient to supply negative charges for the dye adsorption, since this might alter the composition of the solution (Izan et al., 2022). It is evident that when the PPAC rose from 0.0163 to 0.838 g, the adsorption capacity dropped from 362.6 to 118.2 mg/g.

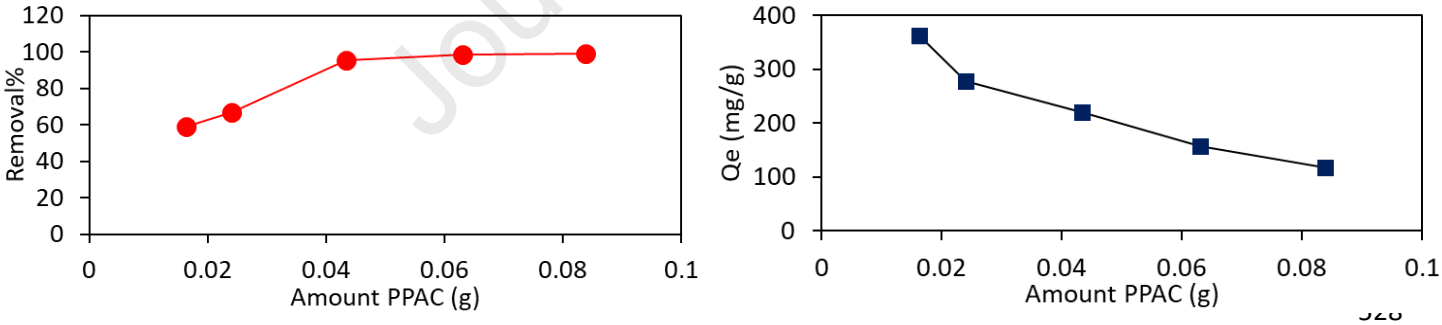

Fig. 4. Impact of PPAC dose (pH 7, 200 mg/L MB, 50 mL, 100 min) on PPAC-adsorbed MG removal efficiency (left hand) and adsorption capacity (right hand)

3.3.4. Effect of solution volume

PPAC shows excellent removal efficiency in the adsorption of the MG dye at various volumes of solution (25, 50, and 100 mL), with the exception of 100 mL.

With using a 25 mL volume, the maximum clearance rate was 100%. The removal efficiency decreases with increasing MG dye solution volume. The maximum adsorption capacity of 231.5 mg/g was achieved with 100 mL of dye solution. **Table 1** and **Figure 5** present these findings.

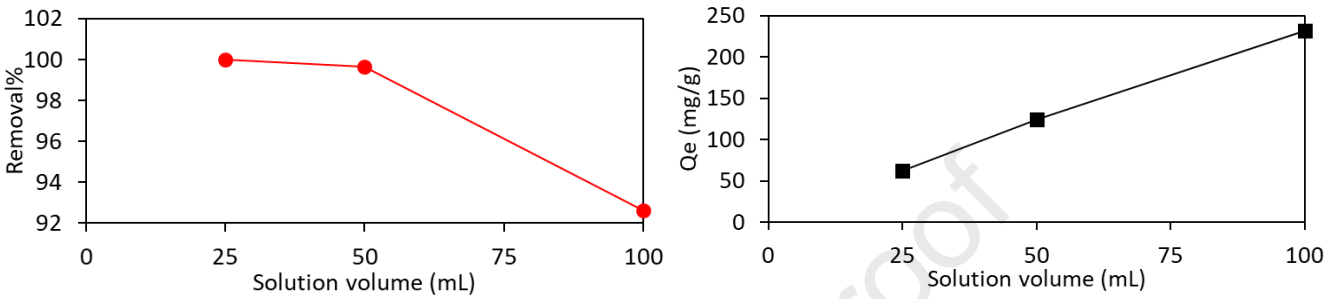

Fig. 5 Impact of the MG solution volume (pH 7, 100 mg/L MB, 0.04 g, 100 min) on the MG adsorption capacity and removal efficiency using PPAC

3.3.5. Effect of temperature

Figure 6 and **Table 1** display the changes in MG adsorption, removal efficiency, and capacity of pomegranate peel activated carbon at different temperatures. At 20 °C, PPAC's elimination efficiency is 92.1%. The removal efficiency can reach 99% at 50 °C. As the temperature increased, the dye molecules' mobility changed, and new active sites for adsorption appeared (Bharathi and Ramesh, 2013). From 20 °C to 50 °C, the adsorption capacity grew steadily with temperature. The maximum adsorption capacity for MG dye adsorption is 247.5 mg/g at 50 °C, while the lowest value is 230.25 mg/g at 20 °C. According to the data shown, a temperature rise results in swelling of the adsorbent's internal structure, which increases the adsorption capacity and permits more penetration of MG (Hu et al., 2018).

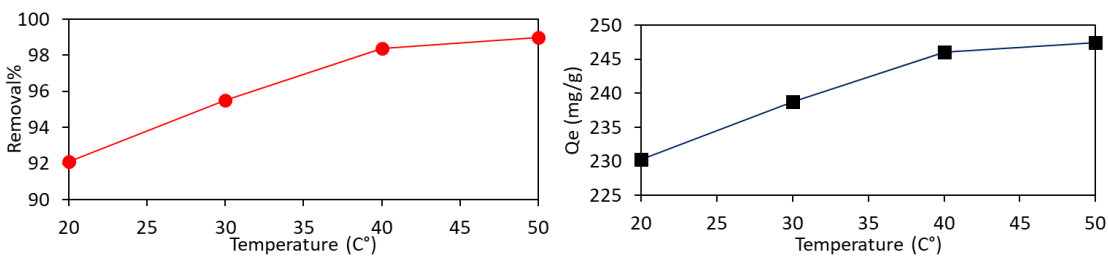

Fig. 6 Impact of temperature on the adsorption capacity and removal efficiency of MG using PPAC (200 mg/L MB, pH 7, 0.04 g adsorbent, 50 mL, 100 min)

3.3.6 Effect of NaCl

The effect of NaCl on the removal efficiency of MG dye by the PPAC adsorbent was evaluated, and the results are shown in **Figure 7**. It is evident that both the removal percentage and adsorption capacity of MG dye decreased in the presence of NaCl. This reduction can be attributed to the increased ionic strength of the aqueous medium caused by the addition of NaCl, which shields the surface-active sites. The presence of positively charged Na^+ ions may reduce the negative charge on the adsorbent's active sites, thereby weakening the electrostatic interactions between the dye molecules and the negatively charged adsorption sites (Mahmoodi et al., 2011; Salah Omer et al., 2022).

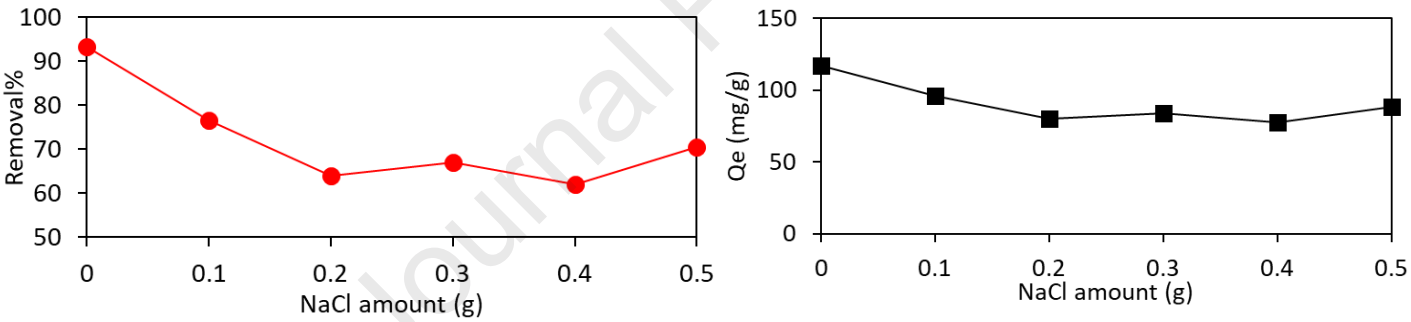

Fig. 7 Impact of NaCl amount on the adsorption capacity and removal efficiency of MG using PPAC (100 mg/L MB, pH 7, 0.04 g adsorbent, 50 mL, 100 min).

Table 1. Removal% and adsorption capacity (Q) under the effect of all selected parameters for the adsorption of MG on PPAC

	Effect of initial concentration (mg/L) [a]				
	30	**60**	**100**	**200**	**300**
R%	100	100	98.3	51	30
Q (mg/g)	37.5	75	122.9	127.5	112.5

	Effect of contact time (min) [b]					
	20	**30**	**40**	**60**	**100**	**120**
R%	78.2	82	85	89	95	96
Q (mg/g)	97.75	102.5	106.25	111.25	118.75	120
	Effect of temperature (°C) [c]					
	20	**30**	**40**	**50**		
R%	92.1	95.5	98.4	99		
Q (mg/g)	230.25	238.75	246	247.5		
	Effect of initial pH solution [d]					
	3	5	7	9	11	
R%	9.4	19.5	97.6	99.12	99.85	
Q (mg/g)	11.75	24.4	122	123.9	124.8	
	Effect of PPAC amount (g) [e]					
	0.0163	0.024	0.0433	0.063	0.0838	
R%	59.1	66.85	95.6	98.6	99.04	
Q (mg/g)	362.6	278.54	220.8	156.5	118.2	
	Effect of volume (mL) [f]					
	25	50	100			
R%	100	99.63	92.6			
Q (mg/g)	62.5	124.5	231.5			
	Effect of NaCl (g)[g]					
	0	0.1	0.2	0.3	0.4	0.5
R%	93.4	76.6	64.1	67	62.1	70.6
Q (mg/g)	116.75	95.75	80.12	83.75	77.62	88.25

[a] 100 min, 50 mL solution, 0.04 g PPAC, pH 7; [b]100 mg/L MG , 50 mL solution, 0.04 g PPAC, pH 7; [c] 100 min, 0.04 g PPAC, 200 mg/L MG, 50 mL solution; [d]100 min, 50 mL solution, 0.04 g PPAC; [e] 100 min, 50 mL solution, 200 mg/L, pH 7; [f] 100 min, 100 mg/L, 0.04 g PPAC, pH 7; [g] 100 min, 50 mL solution, 100 mg/L, pH 7.

3.4. Adsorption isotherm

As can be seen in **Figures 8a and b**, adsorption isotherms were evaluated using the Freundlich and Langmuir models. The best curve fit was chosen after taking the coefficient of determination (R^2) into account. In comparison to the

Langmuir isotherm model, it is determined that the Freundlich isotherm has a maximum R^2 of 0.9996. Moreover, the efficiency of the adsorption process was demonstrated by the determination of the maximum Langmuir adsorption capacity (Q_m) and the Langmuir constant associated with the free energy of adsorption (KL), which were determined to be 126 mg/g and 0.033 L/mg, respectively. However, as shown in **Table 2**, the values of the Freundlich constant (KF) and an empirical parameter associated with intensity (n) were found to be 35.2 and 0.188, respectively. For the adsorption of MG onto PPAC, Figure 8c shows the plot of ln Qe versus ε^2. The slope and intercept of the plot were used to calculate the Dubinin–Radushkevich (D–R) constants: the sorption energy constant (K_{ad}) measured in $mol^2\,kJ^{-2}$ and the maximum adsorption capacity (Qmax) measured in mol g^{-1}. These values are presented in Table 2. The mean free energy of adsorption (E) was also calculated based on the K_{ad} values, and the results are also shown in Table 2. The data indicate that the adsorption energy at 298 K for MG adsorption onto PPAC is less than 8 kJ mol^{-1}, suggesting that the process is mainly driven by physical adsorption forces. The R^2 value obtained from the Dubinin–Radushkevich isotherm is lower than those from other adsorption isotherm models (R^2= 0.3648), indicating that the adsorption of MG onto the PPAC adsorbent does not fit the Dubinin–Radushkevich isotherm well.

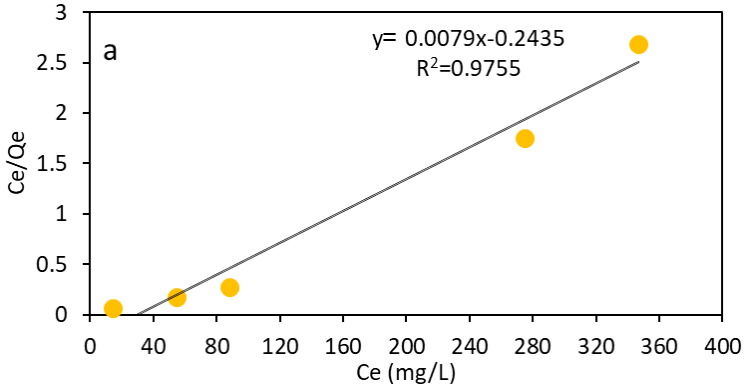

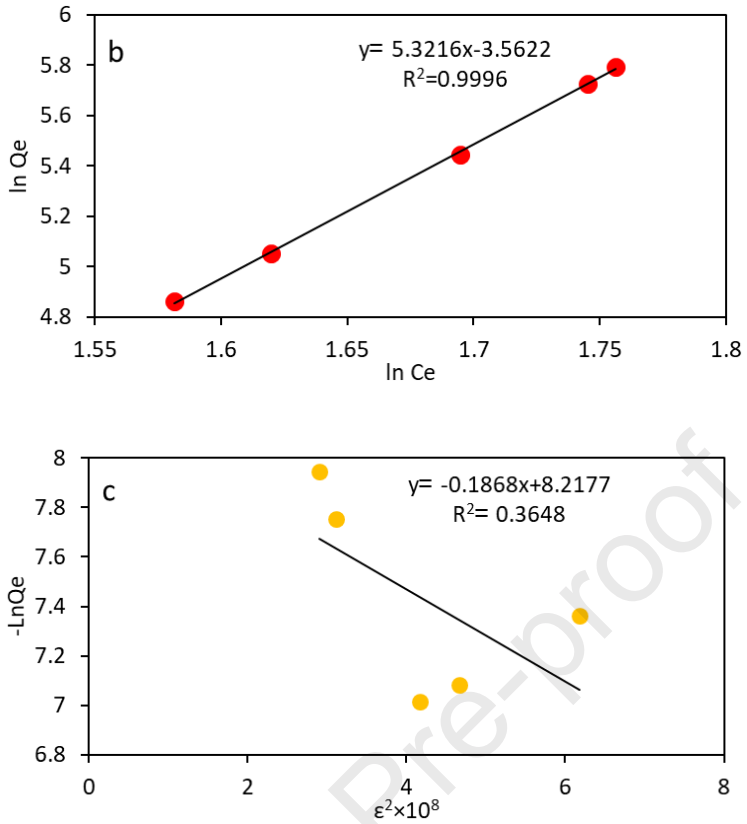

Fig. 8 Isotherm plots (a) Langmuir, (b) Freundlich, and (c) Dubinin–Radushkevich (D–R) for adsorption of MG on PPAC

Table 2. Isotherm parameters for Langmuir and Freundlich models after the adsorption of MG on PPAC

Langmuir isotherm		
Qm (mg/g)	**KL (L/mg)**	**R²**
126	0.033	0.9755
Freundlich isotherm		
KF (mg/g)(L/mg)$^{1/n}$	**n**	**R²**
35.2	0.188	0.9996
Dubinin–Radushkevich isotherm		
E (kJ/mol)	**Qm (mol/g)**	**R²**

16.36	2.7×10^{-4}	0.3648

646

3.5. Adsorption kinetics

647

PFO and PSO models were used to develop the adsorption kinetics model, which is important for assessing the time dependency of dye adsorption and for finding the probable rate-determining step. **Figure 9a,b** and **Table 3** display the pseudo-first-order and pseudo-second-order models, respectively, for the adsorption kinetic processes. The parameter values for each model are shown. The data are shown to fit the pseudo-second-order model (R^2=1) properly when compared to the correlation coefficients found for the pseudo-first-order model. MG dye adsorption onto pomegranate peel-activated carbon is typically governed by a chemical reaction, with the rate of the adsorption process determined by both the adsorbent and the adsorbate (Al-Jaaf et al., 2022). The superior performance of AC (PPAC) as an adsorbent is further supported by the rate constants presented in **Table 3**. It has been observed that the adsorption rate constants for various dyes, such as methylene blue, on waste fig leaves is relatively close (Al-Asadi and Al-Qaim, 2023). As shown in Equation (7), Weber and Morris developed a linearized equation based on the relationship between Q_t vs $t^{1/2}$. The boundary layer effect can be evaluated using the intercept of the IPD graph. The graphs in **Figure 9c** represent the fitting of kinetic data obtained under specific conditions to the linearized Weber and Morris intra-particle diffusion (IPD) model. According to Equation (7), the high R^2 value indicates the model's strong validity. Furthermore, the positive intercept (107.9) from the linear plot is proportional to the thickness of the boundary layer; a larger intercept suggests a greater influence of the boundary layer on the adsorption process (Kaur et al., 2013; Rathnayaka et al., 2024). Diffusion coefficients can be calculated from the slopes of the IPD model, enhancing its analytical capabilities and offering an additional practical application. However, one of

648 649 650 651 652 653 654 655 656 657 658 659 660 661 662 663 664 665 666 667 668 669 670 671 672

the limitations of the IPD model is the complexity involved in applying it to real-samples (Dharmarathna and Priyantha, 2024).

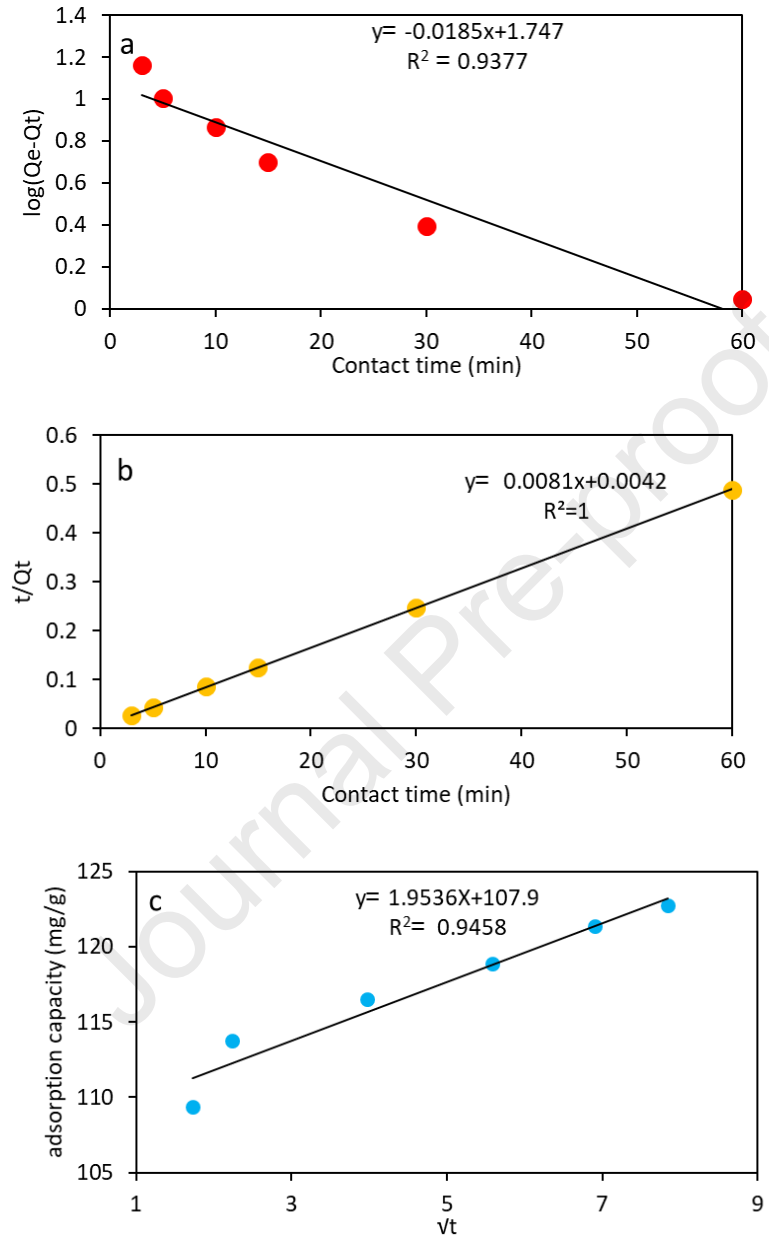

Fig. 9 Investigation of adsorption process kinetics: (a) Plots of the pseudo-first order model log(Qe - Qt) against time; (b) the pseudo-second order model t/Qt versus time, and (c) Plot of the Weber and Morris intra-particle diffusion (IPD) model Qe against the square root of contact time

Table 3. Kinetic parameters of adsorption of MG on PPAC

Pseudo-first-order constant		Pseudo-second-order constant		Intraparticle diffusion constant	
K_{ads1} (min^{-1})	R^2	K_{ads2} (g/min. mg)	R^2	K_{diff} ($g./mg.min^{1/2}$)	R^2
0.0426	0.9377	0.0167	1	1.9536	0.9458

3.6. Adsorption thermodynamics

The energy related to the adsorption process may be found using the adsorption thermodynamics. Determining whether the adsorption is spontaneous or non-spontaneous also aids in this process. In general, the adsorption process is classified as non-spontaneous if the system's Gibbs free energy is positive and as spontaneous if it becomes negative. According to **Table 4 and Figure 10**, the pomegranate peel-AC used to remove the MG dye from an aqueous solution was discovered to be both endothermic (ΔH =58.9 kJ/mol) and thermodynamically spontaneous ($\Delta G < 0$). From a thermodynamic standpoint, it is generally possible for MG dye to be adsorbed onto activated carbon obtained from pomegranate peels.

Table 4: Thermodynamic parameters values for the adsorption of MG onto PPAC at different temperatures

Temperature (K)	Thermodynamic parameters			
	Kd	ΔG° (kJ/mol)	ΔH° (kJ/mol)	ΔS° (J/mol.K)
293	11.658	-5.87	58.9	221.04
303	21.222	-8.08		
313	61.5	-10.29		
323	99	-12.5		

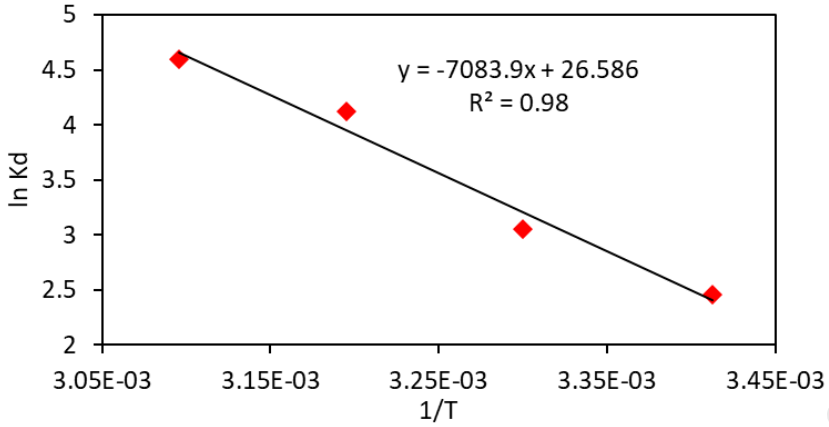

Fig. 10 Curve of the relationship between distribution coefficient and inverse of temperature

The maximal monolayer adsorption capacity of MG dye produced using the AC generated from different peels of agricultural by-products is compared in **Table 5**. In comparison to several earlier studies, PPAC produced comparatively substantial MG dye adsorption.

Table 5 Experimental conditions and maximum adsorption capacity for numerous fruit peels as a low-cost adsorbent for the adsorption of MG compared with PPAC

Fruit Peels-source	**Reagent used**	**MG concentration range (mg/L)**	**AC/solution (g/mL)**	**Treatment time (min)**	**(Q_{max}) mg/g**	**References**
Pomegranate peel	KOH	200 mg/L	0.016 g/50 mL	60 min	362*	The present study
Rambutan peel	KOH	200 mg/L	0.2 g/250 mL	3 h	329	(Ahmad and Alrozi, 2011)
Mandarin peel	No chemical reagent used	200 mg/L	0.05 g/50 mL	150 min	180	(Yalvaç and Bayrak, 2020)
Durian peel	KOH	300 mg/L	0.2 g/200 mL	6 h	211	(Yusop et al., 2021)
Potato peel	No chemical reagent used	50 mg/L	0.05 g/50 mL	120 min	37.8	(Küçük and Biçiçi, 2024)
Mangosteen Peel	H_2SO_4	100 mg/L	0.05 g/25 mL	120 min	29.6	(Yuningsih et al., 2024)
Peel of cassava	No chemical reagent used	40 mg/L	0.02 g/ 200 mL	180 min	92.6	(Belcaid et al., 2024)

* Under these conditions: 0.016g PPAC, 200 mg/L and 50 mL

3.7. Adsorption mechanisms

The adsorption of MG in this particular study is a surface phenomenon, meaning that it occurs spontaneously and promotes the formation of an adsorbate layer on the surface of an activated carbon adsorbent made from pomegranates because of the adhesion of MG molecules from wastewater. The adsorption mechanism involves molecular interactions, transfer of dye molecules across the boundary layer, intraparticle transport into the interior of the sorbent (either by monolayer or multilayer), and adsorption on the surface of the adsorbent. The first step in the adsorption process is the migration or dispersion of pollutants present in water into the porous spaces of carbon particles. While within the pore, mild electrostatic forces known as the Vander Walls force hold the impurity molecules in the interior pore surfaces (Abewaa et al., 2023; Liu et al., 2017). Adsorption is the process of removing solutes from a solution until the solute concentration at the surface and the quantity of solute still in solution are equal. The process of adsorption on AC's surface is typically attributed to the micropores that are present there or the weak van der Waals forces that might draw impurities. These interactions are the outcome of particular interactions between functional groups through the development of donor-acceptor complexes (Liu et al., 2017). However, the FTIR band shifts before and after adsorption, 3423.26 cm^{-1} to 3396.35 cm^{-1}, 1574.95 cm^{-1} to 1573.54 cm^{-1}, 1040.99 cm^{-1} to 1039.58 cm^{-1}, and 650.09 cm^{-1} to 645.84 cm^{-1}, indicating that carboxyl, O-H, C=O, C=C, and C–O were significant factors in the adsorption process. In conclusion, the hydrophobicity of the impurity molecule and the foreign molecule's attraction to carbon, or both, promote the adsorption of contaminants from wastewater.

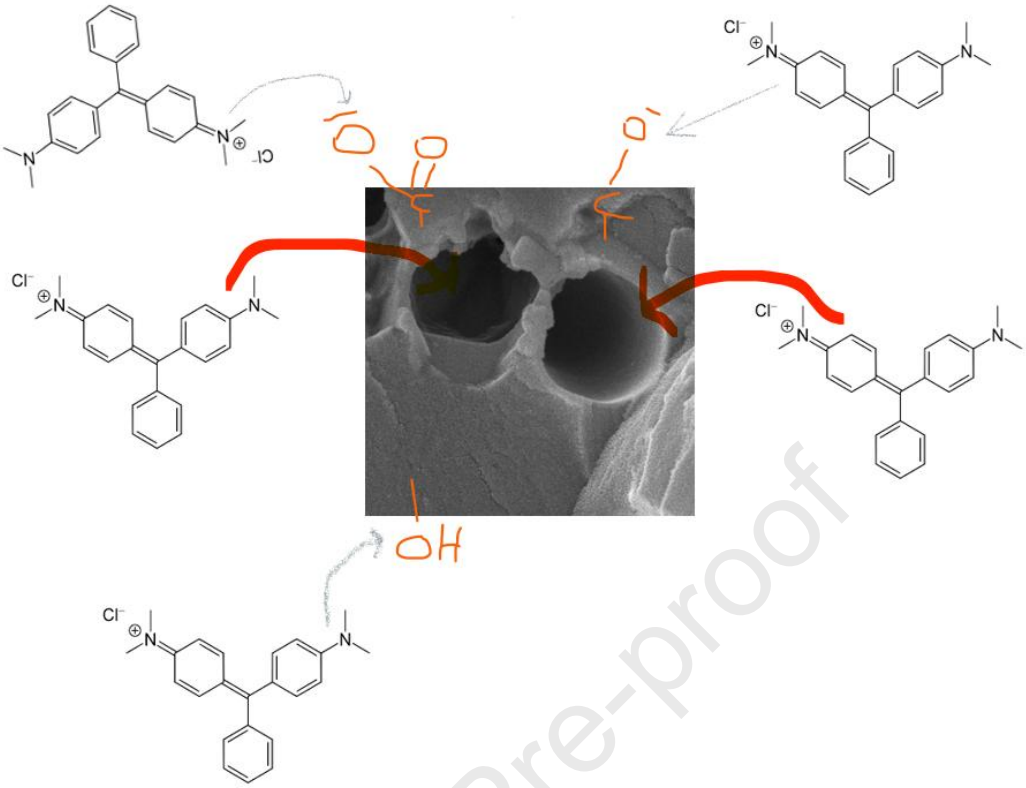

Fig. 11 Proposed mechanism of adsorption of MG on the PPAC surface adsorbent

3.8 Regeneration of the Adsorbent

Adsorption is always followed by desorption, a temporary phase that precedes regeneration. Given environmental concerns and the need for sustainable development, regeneration is a critical factor in evaluating the reusability of any adsorbent for industrial applications. Various chemical, thermal, microbiological, and electrochemical methods can be used to recycle the adsorbent. However, owing to its lower cost, chemical regeneration was selected for this study. Five eluents, water, 0.1 M HCl, methanol, acetic acid: H_2O (1:1), and acetic acid, were used to evaluate the desorption efficiency of the PPAC adsorbent following the adsorption of 50 mL of MG solution at 50 mg/L using 0.1 g of adsorbent in a column cartridge. All columns were rinsed with water after MG adsorption and left to dry overnight. During the desorption test, each eluent was passed through the column individually (see

Figure 12). As shown in **Figure 13**, only 7% and 44% of the dye were desorbed using distilled water and 0.1 M HCl, respectively. However, the desorption efficiency significantly increased to 92% when methanol was used. A variety of eluents for dye desorption were used to investigate the ability of reused activated carbon. However, acetone, acetic acid, methanol, ethanol, ultrapure water, KOH, and HCl exhibited different desorption (Al-Musawi and Al-Qaim, 2024).

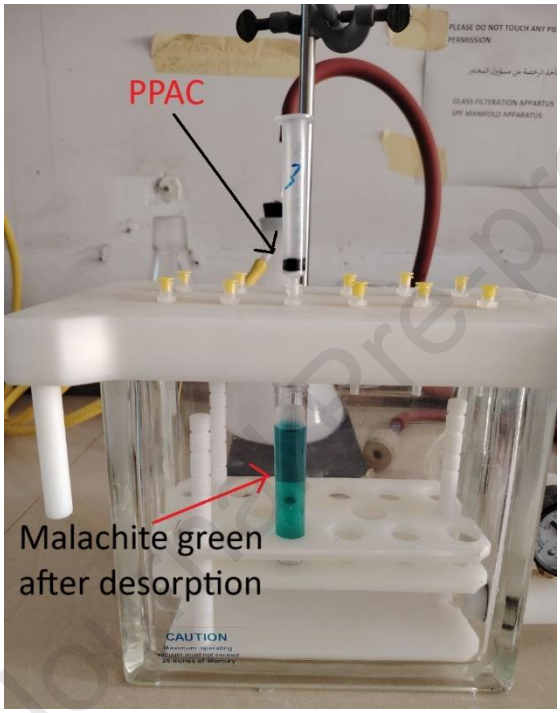

Fig. 12 Desorption of MG with acetic acid using column bed PPAC.

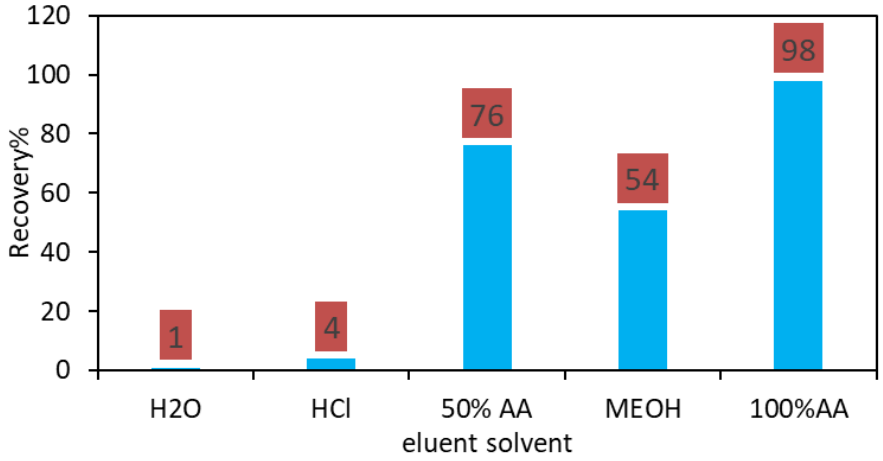

Fig. 13 Assessment of the eluent solvent based on the recovery of MG dye using PPAC

Acetic acid was used as the eluent in three adsorption–desorption cycles (**Figure 14**). PPAC maintained an adsorption efficiency between 98% and 91% during the first two cycles. However, it began to decline in the third cycle, dropping to 84%, and eventually decreased to 76% by the end of the fourth cycle. One of the observed issues was that the eluent persistently occupied several adsorption sites, which explains the decline in adsorption efficiency after a certain number of cycles.

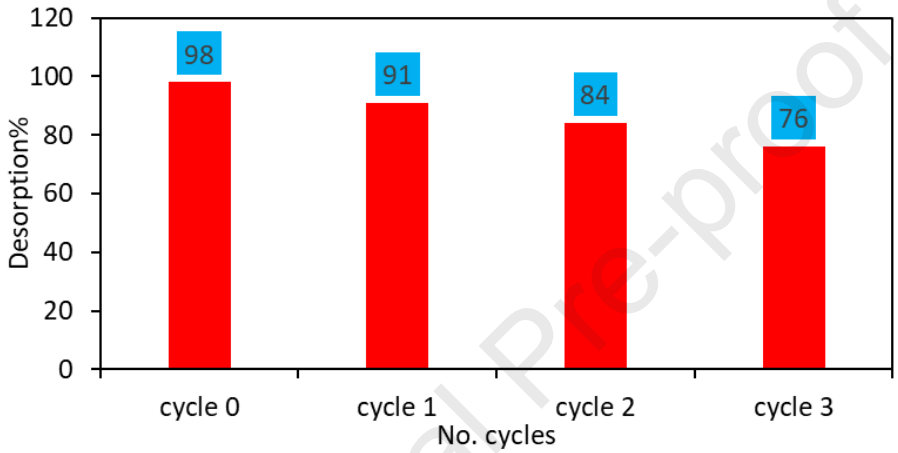

Fig. 14 Regeneration of PPAC using concentrated acetic acid

3.9. **Selectivity dye adsorption**

Regarding the selectivity of pomegranate peels for different dyes, the efficiency of the prepared peels was evaluated under fixed conditions using several dyes: methylene blue, crystal violet, safranin, and the target dye, i.e., MG. It was observed that the activated pomegranate peels (PPAC) play a significant role in dye removal even at high concentrations and demonstrate the capability to adsorb dyes with different chemical properties. The peels were effective in removing not only MG but also methylene blue, crystal violet, and safranin. For this evaluation, a constant weight of PPAC (0.06 g) was used with a fixed dye concentration of 50 mg/L and a volume of 50 mL for each dye. The samples were subjected to shaking for 100 min to maximize adsorption onto the PPAC surface. The results showed that dye removal rates were generally high, with

safranin being the lowest at 70%, while the others ranged between 89% and 94%. These results are considered acceptable and indicate that PPAC has strong potential for removing a range of dyes, not just MG, as illustrated in **Figure 15**. To assess the remaining dye concentrations after adsorption, it is important to note that each dye has a specific absorbance wavelength. Therefore, post-adsorption measurements were performed individually using the characteristic wavelengths for each dye: MG (615 nm), methylene blue (665 nm), crystal violet (590 nm), and safranin (520 nm).

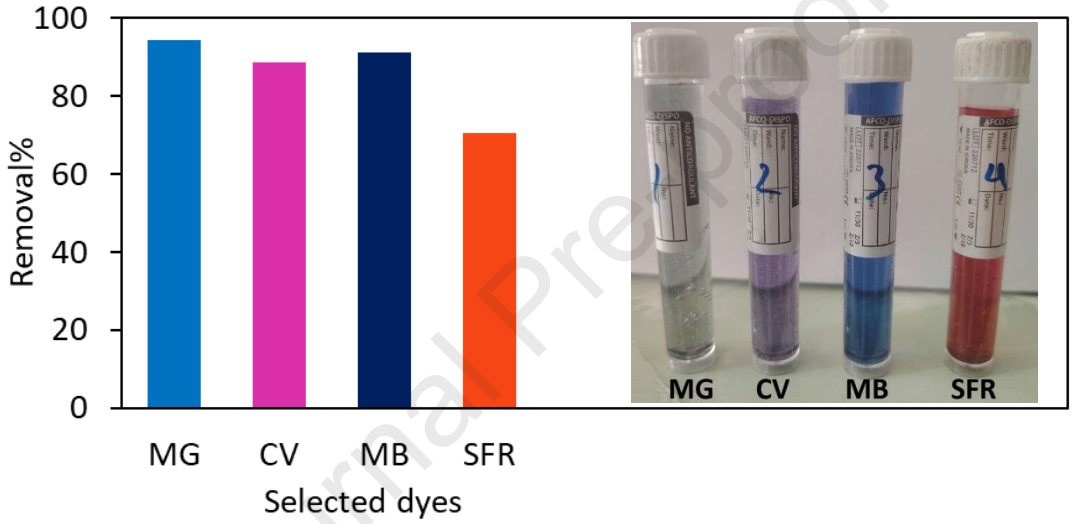

Fig. 15. (Right hand) Adsorption profile for different dyes (MG, CV, MB and SFR) on PPAC adsorbent, **(Left hand)** real photos for the selected dyes after adsorption under these conditions: (50 mg/L dye, 0.06 g adsorbent dose, and 100 min shaking time)

4. Conclusions

The AC obtained from pomegranate peels was produced by chemical and thermal activation, and its SEM, FTIR, BET, and XRD characteristics were assessed. The study revealed a BET-specific surface area of 46 m^2/g. However, FTIR analysis revealed the existence of many functional groups that participate strongly in trapping the dye. Furthermore, the adsorbent's heterogeneous surface and amorphous nature were shown by XRD and SEM investigation.

Throughout the course of the investigation, removal efficiency was shown to range from 9.4 to 100%. At 200 mg/L, 16.3 mg, pH 7, and 100 min, the greatest dye removal efficiency and adsorption capacity of 99.85% and 362.6 mg/g were recorded under testing circumstances. This study carefully investigated the impact of several experimental parameters, including pH, contact duration, adsorbent dose, and starting dye concentration. The purpose of the adsorption isotherm, kinetics, and thermodynamics investigations was to ascertain the kind of adsorption, the mechanism, and the heat transfer related to the adsorption process. Consequently, it was discovered that the pseudo second order reaction kinetics model, with a maximum R^2 value of 1.0000, was descriptive. This demonstrated that the adsorption mechanism was homogeneous surface chemosorption, where a single attachment of contaminants saturated the adsorbent's surface. Thermodynamic studies indicate that adsorption is endothermic and occurs spontaneously. Ultimately, this study demonstrated that activated carbon made from pomegranate peels is a viable option for decolorizing textile effluents. To improve adsorption capacity, it is advised to examine the column analysis and functionalize the adsorbent's surface.

Acknowledgments

The authors thank the College of Sciences for Women, University of Babylon, for facilitating this work. Also, the appreciation for the support from University Al-Ameed and University AlzaHraa.

Contribution statement:

Zainab Haider Mussa: Writing – original draft, Visualization, Methodology, Investigation, Conceptualization**. Ahmed Falah Imran**: Writing – review & editing, Validation, Supervision, Resources, Formal analysis, Conceptualization. **Lubna Raad Al-Ameer**: Writing – original draft, Methodology, Investigation, Formal analysis, Conceptualization. **Haider Falih Shamikh Al-Saedi**: Writing – original draft, Project administration, Methodology, Investigation, Formal analysis, Conceptualization. **Issa Farhan Deyab**: Writing – original draft, Visualization, Software, Formal analysis. **Fouad Fadhil Al-Qaim**: Writing – review & editing, Visualization, Data curation. **Hesam Kamyab**: Writing – review & editing, Visualization, Data curation.

References

Abate, G.Y., Alene, A.N., Habte, A.T., Getahun, D.M., 2020. Adsorptive removal of malachite green dye from aqueous solution onto activated carbon of Catha edulis stem as a low cost bio-adsorbent. Environmental Systems Research 9, 1–13.

Abbas, M., Trari, M., 2023. Contribution of zeolite to remove malachite green in aqueous solution by adsorption processes: Kinetics, isotherms and thermodynamic studies. Textile Research Journal 93, 3765–3776.

Abbasi, F., Mansouri, M., Tanzifi, M., Ebrahimi, F., Sadeghizadeh, A., 2024. The modified pomegranate peel as an economical and highly effective adsorbent for malachite green dye removal from wastewater. Colloids and Surfaces C: Environmental Aspects 2, 100040. https://doi.org/10.1016/j.colsuc.2024.100040

Abbood, N.S., Ali, N.S., Khader, E.H., Majdi, H.S., Albayati, T.M., Saady, N.M.C., 2023. Photocatalytic degradation of cefotaxime pharmaceutical compounds onto a modified nanocatalyst. Research on Chemical Intermediates 49, 43–56.

Abdel-Salam, F.F., El_deen Moharram, Y.G., El-Zalaki, E.M., 2018. Characterization of wastes from pomegranate (Punica granatum L.) juice and its use as a functional drink. Egypt J. Food Sci 46, 91–100.

Abdulhameed, A.S., Al Omari, R.H., Althahban, S., Jazaa, Y., Abualhaija, M., Algburi, S., 2025. Green vegetable waste composited with chitosan as a bioadsorbent for effective removal of methylene blue dye from water: Insight into physicochemical and adsorption characteristics. Biomass Bioenergy 193, 107528. https://doi.org/10.1016/j.biombioe.2024.107528

Abewaa, M., Mengistu, A., Takele, T., Fito, J., Nkambule, T., 2023. Adsorptive removal of malachite green dye from aqueous solution using Rumex abyssinicus derived activated carbon. Sci Rep 13, 14701.

Abid, L.H., Mussa, Z.H., Deyab, I.F., Al-Ameer, L.R., Al-Saedi, H.F.S., Al-Qaim, F.F., Kamyab, H., Rajendran, S., Imran, A.F., Yaseen, Z.M., 2025. Walnut Shell as a bio-activated carbon for elimination of malachite green from its aqueous solution: Adsorption isotherms, kinetics and thermodynamic studies. Results Chem 102124.

Abuzerr, S., Darwish, M., Mahvi, A.H., 2018. Simultaneous removal of cationic methylene blue and anionic reactive red 198 dyes using magnetic activated carbon nanoparticles: equilibrium, and kinetics analysis. Water Science and Technology 2017, 534–545.

Ahmad Khan, F., Dar, B.A., Farooqui, M., 2023. Characterization and adsorption of malachite green dye from aqueous solution onto Salix alba L.(Willow tree) leaves powder and its respective biochar. Int J Phytoremediation 25, 646–657.

Ahmad, M.A., Alrozi, R., 2011. Removal of malachite green dye from aqueous solution using rambutan peel-based activated carbon: Equilibrium, kinetic and thermodynamic studies. Chemical Engineering Journal 171, 510–516.

Al-Asadi, S.T., Al-Qaim, F.F., 2023. Application of response surface methodology on efficiency of fig leaf activated carbon for removal of methylene blue dye. Eurasian Chem. Commun. 5, 794–811.

Al-Asadi, S.T., Al-Qaim, F.F., Al-Saedi, H.F.S., Deyab, I.F., Kamyab, H., Chelliapan, S., 2023. Adsorption of methylene blue dye from aqueous solution using low-cost adsorbent: kinetic, isotherm adsorption, and thermodynamic studies. Environ Monit Assess 195, 676.

Al-Asadi, S.T., Mussa, Z.H., Al-Qaim, F.F., Kamyab, H., Al-Saedi, H.F.S., Deyab, I.F., Kadhim, N.J., 2025. A comprehensive review of methylene blue dye adsorption on activated carbon from edible fruit seeds: A case study on kinetics and adsorption models. Carbon Trends. https://doi.org/10.1016/j.cartre.2025.100507

Ali, N.S., Alismaeel, Z.T., Majdi, H.S., Salih, H.G., Abdulrahman, M.A., Saady, N.M.C., Albayati, T.M., 2022. Modification of SBA-15 mesoporous silica as an active heterogeneous catalyst for the hydroisomerization and hydrocracking of n-heptane. Heliyon 8.

Al-Jaaf, H.J., Ali, N.S., Alardhi, S.M., Albayati, T.M., 2022. Implementing eggplant peels as an efficient bio-adsorbent for treatment of oily domestic wastewater. Desalin. Water Treat 245, 226–237.

Al-Musawi, E.B., Al-Qaim, F.F., 2024. Elimination of methylene blue dye from the aqueous solution using waste fig fruit as an activated carbon: a case study of nonlinear adsorption isotherm models and kinetic models. Reaction Kinetics, Mechanisms and Catalysis 1–23.

Almuslem, A.S., Alnaim, N., Ibrahim, S.S., Ibrahim, M.A., 2023. Green synthesis and characteristics of cellulose nanocrystal/poly acrylic acid nanocomposite thin film for organic dye adsorption during water treatment. Polymers (Basel) 15, 2154.

Al-Qaim, F.F., Al-Saedi, H.F.S., Mussa, Z.H., Kadhim, N.J., Al-Qaim, Z.H., 2024. Application of the response surface approach to the adsorption of methylene blue from water using acid-modified grape leaves. Reaction Kinetics, Mechanisms and Catalysis 137, 399–422.

Al-Qaim, F.F., Jusof, S.H., Abdullah, M.P., Mussa, Z.H., Tahrim, N.A., Khalik, W.M.A.W.M., Othman, M.R., 2017. Determination of caffeine in surface water using solid phase extraction and high perfomance liquid chromatography. Malaysian Journal of Analytical Sciences 21. https://doi.org/10.17576/mjas-2017-2101-11

Al-Qaim, F.F., Mussa, Z.H., Yuzir, A., Latip, J., Othman, M.R., 2018. The fate of prazosin and levonorgestrel after electrochemical degradation process: Monitoring by-products using LC-TOF/MS. J Environ Sci (China). https://doi.org/10.1016/j.jes.2018.02.019

Amigun, A.T., Adekola, F.A., Tijani, J.O., Mustapha, S., 2022. Photocatalytic degradation of malachite green dye using nitrogen/sodium/iron-TiO2 nanocatalysts. Results Chem 4, 100480.

Barría, Y., Burbano, A., James, A., Gascó, G., Méndez, A., 2023. Sorption capacity of biochars obtained by gasification of rice husks and wild sugarcane: Removal of malachite green and arsenic from water solutions. Biomass Convers Biorefin 1–13.

Belcaid, A., Beakou, B.H., Bouhsina, S., Anouar, A., 2024. Insight into adsorptive removal of methylene blue, malachite green, and rhodamine B dyes by cassava peel biochar (Manihot esculenta Crantz) in single, binary, and ternary systems: competitive adsorption study and theoretical calculations. Biomass Convers Biorefin 14, 7783–7806.

Bharathi, K.S., Ramesh, S.T., 2013. Removal of dyes using agricultural waste as low-cost adsorbents: a review. Appl Water Sci 3, 773–790.

Bhat, S.S., Narayana, B., Bhat, J.I., 2023. Adsorption of malachite green dye using low-cost adsorbent derived from java apple leaves (Syzyium samarangense). Sādhanā 48, 138.

Dharmarathna, S.P., Priyantha, N., 2024. Investigation of boundary layer effect of intra-particle diffusion on methylene blue adsorption on activated carbon. Energy Nexus 14, 100294. https://doi.org/10.1016/j.nexus.2024.100294

Fadhil Al-Qaim, F., Abdullah, P., Rozali Othman, M., n.d. ANALYSIS OF DIFFERENT THERAPEUTIC CLASSES USING LIQUID CHROMATOGRAPHY-MASS SPECTROMETRY IN AQUATIC ENVIRONMENT: A REVIEW.

Fito, J., Ebrahim, O., Nkambule, T.T.I., 2023. The application Mn-Ni ferrite nanocomposite for adsorption of chromium from textile industrial wastewater. Water Air Soil Pollut 234, 37.

Fito, J., Kefeni, K.K., Nkambule, T.T.I., 2022. The potential of biochar-photocatalytic nanocomposites for removal of organic micropollutants from wastewater. Science of the Total Environment 829, 154648.

Genel, Y., Genel, İ., Saka, C., 2024. Facile preparation of sulfonated carbon particles with pomegranate peels as adsorbent for enhanced methylene blue adsorption from aqueous solutions. Biomass Convers Biorefin 14, 30693–30705. https://doi.org/10.1007/s13399-024-05328-4

Giri, R., Kumari, N., Behera, M., Sharma, A., Kumar, S., Kumar, N., Singh, R., 2021. Adsorption of hexavalent chromium from aqueous solution using pomegranate peel as low-cost biosorbent. Environmental Sustainability 4, 401–417.

Hasnaoui, N., Wathelet, B., Jiménez-Araujo, A., 2014. Valorization of pomegranate peel from 12 cultivars: Dietary fibre composition, antioxidant capacity and functional properties. Food Chem 160, 196–203.

He, J., Mo, P., Luo, Y.-S., Yang, P.-H., 2023. Strategies for solving the issue of malachite green residues in aquatic products: A review. Aquac Res 2023, 8578570.

Hu, X.-S., Liang, R., Sun, G., 2018. Super-adsorbent hydrogel for removal of methylene blue dye from aqueous solution. J Mater Chem A Mater 6, 17612–17624.

Humadi, J.I., Jafar, S.A., Ali, N.S., Ahmed, M.A., Mzeed, M.J., Al-Salhi, R.J., Saady, N.M.C., Majdi, H.S., Zendehboudi, S., Albayati, T.M., 2023. Recovery of fuel from real waste oily sludge via a new eco-friendly surfactant material used in a digital baffle batch extraction unit. Sci Rep 13, 9931.

Izadmehr, N., Mansourpanah, Y., Ulbricht, M., Rahimpour, A., Omidkhah, M.R., 2020. TETA-anchored graphene oxide enhanced polyamide thin film nanofiltration membrane for water purification; performance and antifouling properties. J Environ Manage 276, 111299.

Izan, N.R., Zainol, M.M., Nordin, A.H., Asmadi, M., Wong, S.L., Azhar, M.A.I., Alias, N.H., 2022. Removal of Methylene Blue via Adsorption using Magnetic Char Derived from Food Waste. Malaysian Journal of Chemistry 24, 283–292.

Jabar, J.M., Adebayo, M.A., Odusote, Y.A., Yılmaz, M., Rangabhashiyam, S., 2023. Valorization of microwave-assisted H3PO4-activated plantain (Musa paradisiacal L) leaf biochar for malachite green sequestration: models and mechanism of adsorption. Results in Engineering 18, 101129.

Jabbar, N.M., Alardhi, S.M., Mohammed, A.K., Salih, I.K., Albayati, T.M., 2022. Challenges in the implementation of bioremediation processes in

petroleum-contaminated soils: A review. Environ Nanotechnol Monit Manag 18, 100694.

Jani, N.A., Haddad, L., Abdulhameed, A.S., Jawad, A.H., ALOthman, Z.A., Yaseen, Z.M., 2024. Modeling and optimization of the adsorptive removal of crystal violet dye by durian (Durio zibethinus) seeds powder: insight into kinetic, isotherm, thermodynamic, and adsorption mechanism. Biomass Convers Biorefin 14. https://doi.org/10.1007/s13399-022-03319-x

Jasim, N.A., Ammar, S.H., Ebrahim, S.E., 2024. Assembling ZnMnFe2O4@Ag-AgVO3 nanostructure heterojunctions for photocatalytically degrading RhB and Pseudomonas aeruginosa bacteria under visible irradiation. J Photochem Photobiol A Chem 449. https://doi.org/10.1016/j.jphotochem.2023.115380

Karaouzas, I., Kapetanaki, N., Mentzafou, A., Kanellopoulos, T.D., Skoulikidis, N., 2021. Heavy metal contamination status in Greek surface waters: A review with application and evaluation of pollution indices. Chemosphere 263, 128192.

Kaur, S., Rani, S., Mahajan, R.K., 2013. Adsorption Kinetics for the Removal of Hazardous Dye Congo Red by Biowaste Materials as Adsorbents. J Chem. https://doi.org/10.1155/2013/628582

Khadim, A.T., Albayati, T.M., Saady, N.M.C., 2022. Removal of sulfur compounds from real diesel fuel employing the encapsulated mesoporous material adsorbent Co/MCM-41 in a fixed-bed column. Microporous and Mesoporous Materials 341, 112020.

Küçük, İ., Biçiçi, H., 2024. Adsorption of malachite green into potato peel: nonlinear isotherm and kinetic. Konya Journal of Engineering Sciences 12, 150–161.

Kumar, E., Bhatnagar, A., Hogland, W., Marques, M., Sillanpää, M., 2014. Interaction of anionic pollutants with Al-based adsorbents in aqueous media–A review. Chemical Engineering Journal 241, 443–456.

Laskar, N., Herbert, A., Kumar, U., 2023. Application of Taguchi methodology in adsorption of malachite green dye using chemically enhanced Bambusa tulda (Indian timber bamboo). Advances in Environmental Technology 9, 99–111.

Lemos, E.S., Fiorentini, E.F., Bonilla-Petriciolet, A., Escudero, L.B., 2023. Malachite green removal by grape stalks biosorption from natural waters and effluents. Adsorption Science & Technology 2023, 6695937.

Lin, H., Zhang, M., 2023. Advanced membrane technologies for wastewater treatment and recycling. Membranes (Basel).

Liu, G., Li, X., Campos, L.C., 2017. Role of the functional groups in the adsorption of bisphenol A onto activated carbon: thermal modification and mechanism. Journal of Water Supply: Research and Technology—AQUA 66, 105–115.

Liu, L., 2021. The use of GIS-based genetic algorithm in water pollution control planning. Desalination Water Treat 241, 223–229.

Mahmoodi, N.M., Salehi, R., Arami, M., Bahrami, H., 2011. Dye removal from colored textile wastewater using chitosan in binary systems. Desalination 267. https://doi.org/10.1016/j.desal.2010.09.007

Merrad, S., Abbas, M., Trari, M., 2023. Adsorption of malachite green onto walnut shells: Kinetics, thermodynamic, and regeneration of the adsorbent by chemical process. Fibers and Polymers 24, 1067–1081.

Mohamed, F.F., Allah, P.M.A., Mehdi, A., Baseem, M., 2011. Photoremoval of Malachite Green (MG) using advanced oxidation process. Res J Chem Environ 15.

Mussa, Z.H., Al-Saedi, H.F.S., Kadhim, N.J., Al-Qaim, Z.H., Al-Qaim, F.F., Kamyab, H., 2024. Electrochemical degradation of carbamazepine-10,11-epoxide through a reactive intermediate "hypochlorite ions": A case study of monitoring the by-products using LC-TOF/MS. Talanta Open 10. https://doi.org/10.1016/j.talo.2024.100385

Oladoye, P.O., Ajiboye, T.O., Wanyonyi, W.C., Omotola, E.O., Oladipo, M.E., 2023. Insights into remediation and decontamination technology of malachite green wastewater. Water Sci. Eng 10.

Olasehinde, E.F., Abegunde, S.M., Adebayo, M.A., 2020. Adsorption isotherms, kinetics and thermodynamic studies of methylene blue dye removal using raphia taedigera seed activated carbon. Caspian Journal of Environmental Sciences 18. https://doi.org/10.22124/cjes.2020.4279

Piriya, R.S., Jayabalakrishnan, R.M., Maheswari, M., Boomiraj, K., Oumabady, S., 2023. Comparative adsorption study of malachite green dye on acid-activated carbon. Int J Environ Anal Chem 103, 16–30.

Raji, Y., Nadi, A., Mechnou, I., Saadouni, M., Cherkaoui, O., Zyade, S., 2023. High adsorption capacities of crystal violet dye by low-cost activated carbon prepared from Moroccan Moringa oleifera wastes: Characterization, adsorption and mechanism study. Diam Relat Mater 135, 109834.

Rathnayaka, R.M.H., Priyantha, N., Gunathilake, W.S.S., 2024. Removal of trivalent and hexavalent chromium from aqueous solution using fiber of Agave americana plant and its modified forms. Colloids and Surfaces C: Environmental Aspects 2. https://doi.org/10.1016/j.colsuc.2024.100029

Ruan, J.-H., Li, J., Adili, G., Sun, G.-Y., Abuduaini, M., Abdulla, R., Maiwulanjiang, M., Aisa, H.A., 2022. Phenolic compounds and bioactivities from pomegranate (Punica granatum L.) peels. J Agric Food Chem 70, 3678–3686.

Salah Omer, A., El Naeem, G.A., Abd-Elhamid, A.I., Farahat, O.O.M., El-Bardan, A.A., Soliman, H.M.A., Nayl, A.A., 2022. Adsorption of crystal violet and methylene blue dyes using a cellulose-based adsorbent from sugercane bagasse: characterization, kinetic and isotherm studies. Journal

of Materials Research and Technology 19. https://doi.org/10.1016/j.jmrt.2022.06.045

Saravanan, A., Deivayanai, V.C., Kumar, P.S., Rangasamy, G., Hemavathy, R. V, Harshana, T., Gayathri, N., Alagumalai, K., 2022. A detailed review on advanced oxidation process in treatment of wastewater: Mechanism, challenges and future outlook. Chemosphere 308, 136524.

Shah, M.I., Javed, M.F., Abunama, T., 2021. Proposed formulation of surface water quality and modelling using gene expression, machine learning, and regression techniques. Environmental Science and Pollution Research 28, 13202–13220.

Singh, B., Singh, J.P., Kaur, A., Singh, N., 2018. Phenolic compounds as beneficial phytochemicals in pomegranate (Punica granatum L.) peel: A review. Food Chem 261, 75–86.

Taqui, S.N., Mohan, C.S., Khatoon, B.A., Soudagar, M.E.M., Khan, T.M.Y., Mujtaba, M.A., Ahmed, W., Elfasakhany, A., Kumar, R., Pruncu, C.I., 2023. Sustainable adsorption method for the remediation of malachite green dye using nutraceutical industrial fenugreek seed spent. Biomass Convers Biorefin 13, 9119–9130.

Waghmare, C., Ghodmare, S., Ansari, K., Alfaisal, F.M., Alam, S., Khan, M.A., Ezaier, Y., 2024. Adsorption of methylene blue dye onto phosphoric acid-treated pomegranate peel adsorbent: Kinetic and thermodynamic studies. Desalination Water Treat 318, 100406. https://doi.org/10.1016/j.dwt.2024.100406

Wang, S., Zhu, Z.H., Coomes, A., Haghseresht, F., Lu, G.Q., 2005. The physical and surface chemical characteristics of activated carbons and the adsorption of methylene blue from wastewater. J Colloid Interface Sci 284. https://doi.org/10.1016/j.jcis.2004.10.050

Wang, T., Zhong, Y., Wang, C., Tong, G., 2021. A low capital method for silicon interference in bamboo kraft pulping alkaline recovery system. J Clean Prod 315, 128283.

Wu, F.C., Tseng, R.L., Juang, R.S., 2009. Initial behavior of intraparticle diffusion model used in the description of adsorption kinetics. Chemical Engineering Journal 153. https://doi.org/10.1016/j.cej.2009.04.042

Xing, L. an, Yang, F., Zhong, X., Liu, Y., Lu, H., Guo, Z., Lv, G., Yang, J., Yuan, A., Pan, J., 2023. Ultra-microporous cotton fiber-derived activated carbon by a facile one-step chemical activation strategy for efficient CO2 adsorption. Sep Purif Technol 324. https://doi.org/10.1016/j.seppur.2023.124470

Yalvaç, G.M., Bayrak, B., 2020. Use of natural and effective mandarin peel in elimination of malachite green from the aqueous media: adsorption properties, kinetics and thermodynamics. Desalination Water Treat 177, 176–185.

Yuningsih, N.E., Ariani, L., Suprapto, S., Ulfin, I., Harmami, H., Juwono, H., Ni'mah, Y.L., 2024. Adsorption of Malachite Green Using Activated Carbon from Mangosteen Peel: Optimization Using Box-Behnken Design. J Renew Mater 12.

Yusop, M.F.M., Ahmad, M.A., Rosli, N.A., Gonawan, F.N., Abdullah, S.J., 2021. Scavenging malachite green dye from aqueous solution using durian peel based activated carbon. Malaysian Journal of Fundamental and Applied Sciences 17, 95–103.

Declaration of interests

☒ The authors declare that they have no known competing financial interests or personal relationships that could have appeared to influence the work reported in this paper.

☐The authors declare the following financial interests/personal relationships which may be considered as potential competing interests: